Neurobiology of Aging 76 (2019) 133–140

Contents lists available at ScienceDirect

Neurobiology of Aging

journal homepage: www.elsevier.com/locate/neuaging

Clinical and biomarker changes in presymptomatic genetic frontotemporal dementia

Alberto Benussi [a], Stefano Gazzina [a], Enrico Premi [b], Maura Cosseddu [b], Silvana Archetti [c], Valentina Dell'Era [a], Valentina Cantoni [a,d], Maria Sofia Cotelli [e], Antonella Alberici [b], Anna Micheli [f], Luisa Benussi [g], Roberta Ghidoni [g], Alessandro Padovani [a], Barbara Borroni [a,*]

[a] Department of Clinical and Experimental Sciences, Neurology Unit, University of Brescia, Brescia, Italy
[b] Department of Neurological Sciences and Vision, Neurology Unit, Brescia Hospital, Brescia, Italy
[c] Department of Laboratory Diagnostics, III Laboratory of Analysis, Brescia Hospital, Brescia, Italy
[d] Department of Neuroscience, Psychology, Drug Research and Child Health, University of Florence, Italy
[e] Neurology Unit, Valle Camonica Hospital, Brescia, Italy
[f] Casa di Cura San Francesco, Bergamo, Italy
[g] Molecular Markers Laboratory, IRCCS Istituto Centro San Giovanni di Dio-Fatebenefratelli, Brescia, Italy

ARTICLE INFO

Article history:
Received 20 November 2018
Received in revised form 28 December 2018
Accepted 30 December 2018
Available online 7 January 2019

Keywords:
Frontotemporal dementia
GRN
C9orf72
Biomarkers
Transcranial magnetic stimulation

ABSTRACT

Presymptomatic carriers of *GRN* and *C9orf72* mutations, the most frequent genetic causes of frontotemporal lobar degeneration, represent the optimal target population for the development of disease-modifying drugs. Preclinical biomarkers are needed to monitor the effect of therapeutic interventions in this population. We assessed clinical, functional, and neurophysiological measures in 113 *GRN* or *C9orf72* carriers and in 73 noncarrier first-degree relatives. For 73 patients, follow-up longitudinal data were available. Differences between carriers and noncarriers were assessed using linear mixed-effects models. We observed that biological changes and intracortical facilitation transmission abnormalities significantly antecede the emergence of clinical symptoms of at least 3 decades. These are followed by intracortical inhibition transmission deficits, detected approximately 2 decades before expected symptom onset and then followed by an increase of white matter lesions, structural brain atrophy, and cognitive impairment. These results highlight how several biomarkers can show different aspects and rates of decline, possibly correlated with the underlying physiopathological process, that arise decades before the onset of clinical symptoms.

1. Introduction

Frontotemporal dementia (FTD) is a genetically and pathologically heterogeneous disorder which can present clinically with personality changes and behavioral symptoms (behavioral variant FTD) (Rascovsky et al., 2011) or language impairment (primary progressive aphasia) (Gorno-Tempini et al., 2011), associated with asymmetrical frontal and temporal lobe degeneration (The Lund and Manchester Groups, 1994).

Mutations within the *microtubule-associated protein tau* (*MAPT*), *granulin* (*GRN*), and the *hexanucleotide repeat expansion of the chromosome 9 open-reading-frame 72* (*C9orf72*) are the main causal genes in autosomal-dominant FTD (Rohrer et al., 2009). These mutations show virtually complete penetrance, and mutation carriers therefore provide a unique window of opportunity to gain insights into the earliest stages of the disease process (Benussi et al., 2015).

Indeed, several studies have now shown that the symptomatic phase is preceded by a long period of gradual accrual of pathological changes; however, the order and timing of processes that lead to clinical FTD are still poorly understood.

Monogenic FTD has a relatively predictable age at onset, mainly defined by mutation type and background family genetics (Rohrer et al., 2015), thus providing a privileged scenario to determine the sequence of preclinical pathological modifications. The identification of preclinical biomarker changes could aid in (1) understanding thoroughly the natural disease course from the onset of the earliest abnormalities to symptom onset, (2) establish possible targets in prevention trials, and (3) determine proper biomarkers to be used as outcome response measures.

* Corresponding author at: Clinica Neurologica, Università degli Studi di Brescia P.le Spedali Civili 1, 25123 Brescia, Italy. Tel.: +39 0303995632; fax: +39 0303995014.
E-mail address: bborroni@inwind.it (B. Borroni).

0197-4580/$ – see front matter © 2019 Elsevier Inc. All rights reserved.
https://doi.org/10.1016/j.neurobiolaging.2018.12.018

Results from the Genetic Frontotemporal dementia Initiative, a multicenter study on the genetic forms of FTD, have identified significant gray matter atrophy and cognitive changes in mutation carriers up to 5–10 years before expected symptom onset (Rohrer et al., 2015). In addition, *GRN* mutation carriers are characterized by an increased load of white matter hyperintensities (WMH) (Le Ber et al., 2008; Paternicò et al., 2016; Pietroboni et al., 2011), with an association of increased WMH volume with expected years from symptom onset (Sudre et al., 2017). *GRN* null mutations cause protein haploinsufficiency, leading to decreased levels of blood and cerebrospinal fluid progranulin; because the reduction of progranulin invariably precedes clinical symptoms, progranulin dosage allows the discrimination of presymptomatic and symptomatic *GRN* mutation carriers from noncarriers with high accuracy regardless of their disease status (Ghidoni et al., 2008; Meeter et al., 2016).

More recently, neurophysiological biomarkers of intracortical connectivity, evaluated with transcranial magnetic stimulation (TMS), have shown that the disruption of functional cortical circuits might even begin before the development of structural imaging changes, at more than 15 years before the onset of clinical symptoms (Benussi et al., 2016; Gazzina et al., 2018). Indeed, it is now widely accepted that FTD is characterized by neurochemical changes that may contribute to the symptomatology of FTD, over and above neuronal loss and atrophy, with particular involvement of GABAergic and glutamatergic neurotransmission (Benussi et al., 2017; Murley and Rowe, 2018).

Altogether, the aforementioned findings suggest a potential series of biomarkers, their usefulness for staging and monitoring disease progression being still a matter of debate. Although changes over time of clinical and neuroimaging biomarkers in at-risk carriers have been previously described, studies which integrate biochemical and neurophysiological functional connectivity measures are currently lacking. These observations defined the objective of this work, aimed at assessing, in a combined model, the different order, rate, and relationship of clinical, behavioral, imaging, biochemical and neurophysiological biomarkers in autosomal-dominant FTD. We compared mutation carriers and noncarriers as a function of the parental age at onset to evaluate the cascade of events that lead to the onset of dementia.

2. Methods

2.1. Study design

Patients with monogenic FTD and family members at risk for carrying a pathogenic mutation for FTD were enrolled. All participants were screened for the presence of pathogenic null mutations in the *GRN* gene and of pathogenic expansion in the *C9orf72* gene, defined as the presence of greater than 30 hexanucleotide repeats. In the present study, 186 participants, from 63 families, were recruited from the Neurology Unit, Department of Clinical and Experimental Sciences, University of Brescia. One hundred eighty-six participants were included in the present study. Excluding plasma progranulin levels, which were evaluated only in *GRN* mutation carriers, all other biomarkers were comprehensively assessed in >85% of the study population. Participants were included in the model only if at least clinical and neuroimaging or neurophysiological biomarkers were available. Moreover, 74 participants were evaluated at subsequent follow-ups, with an average interval between evaluations of 12.5 ± 3.7 months, for a total of 3.0 ± 1.2 evaluations per patient.

The parental age at onset and symptomatic status were determined by a semistructured interview in which family members or close friends were asked about the age of first progressive cognitive decline. Estimated years from expected symptom onset in presymptomatic mutation carriers were calculated as the age of the participant at the time of the study assessment minus the mean familial age at symptom onset, as previously reported (Rohrer et al., 2015). For example, if someone aged 45 years at the time of study assessment with a mean familial age of onset of 60 years (father 58 and brother 62), then the estimated years from expected symptom onset would be −15. Most at-risk participants had not undergone presymptomatic genetic testing and counseling and were therefore unaware of mutation status, as the clinicians performed the various assessments. Full written informed consent was obtained from all participants according to the Declaration of Helsinki. All study procedures were approved by the local ethics committee of the Brescia Hospital, Italy.

2.2. Neuropsychological evaluation

Participants underwent a standardized neuropsychological assessment, but results of only 3 tests are reported here because of space limitations. These tests, which are widely used in FTD research centers, were selected because of their high dissemination and sensitivity in identifying initial cognitive changes in presymptomatic genetic FTD, as previously reported (Rohrer et al., 2015). We considered behavioral symptoms, assessed with the Cambridge Behavioural Inventory-Revised version, general cognitive function evaluated with the Mini-Mental State Examination, and cognitive processing speed assessed with the part A of the Trial Making Test.

2.3. Brain imaging

Brain images were collected using either a 1.5 Tesla (Siemens Avanto, Erlangen, Germany) or a 3 Tesla scanner (Siemens Skyra, Erlangen, Germany) equipped with a circularly polarized transmit-receive coil to obtain 3D magnetization-prepared rapid gradient echo (MPRAGE) T1-weighted scans and fluid-attenuated inversion recovery (FLAIR) T2-weighted scans. At 1.5 T, MPRAGE sequence was acquired with the following parameters: repetition time 2050 ms, echo time 2.56 ms, inversion time 1100 ms, slice thickness 1 mm, voxel size 1 × 1 × 1 mm, in-plane field of view 256 mm, flip angle = 15°. FLAIR sequence parameters were repetition time 8200 ms, echo time 104 ms, inversion time 2500 ms, slice thickness 5 mm, voxel size 1.1 × 0.8 × 5 mm, in-plane field of view 240 mm, flip angle 150°. At 3 T, MPRAGE sequence was acquired with the following parameters: repetition time 2000 ms, echo time 2.92 ms, inversion time 850 ms, slice thickness 1.1 mm, voxel size 1.1 × 1.1 × 1.1, field of view 282 mm, flip angle 8°. FLAIR sequence parameters were repetition time 9000 ms, echo time 81 ms, inversion time 2500 ms, slice thickness 4 mm, voxel size 0.7 × 0.7 × 4 mm, in-plane field of view 220 mm, flip angle 150°. T1 and FLAIR scans were visually inspected and excluded from subsequent analyses if excessive motion blurring or artifacts were present. As the first step, the raw digital imaging and communications in medicine scans were converted into the Neuroimaging Informatics Technology Initiative format, using MRIcroGL software (https://www.nitrc.org/projects/mricrogl/) and reoriented to the anterior commissure using the "Display" function in Statistical Parametric Mapping (SPM12 v.7219) (http://www.fil.ion.ucl.ac.uk/spm/software/spm12/) running on MATLAB 8.5 (The MathWorks, Inc, Natick, MA USA). Then, T1-weighted images were processed and analyzed with the voxel-based morphometry (VBM) pipeline implemented in the Computational Anatomy Toolbox (CAT12 v.1278) (http://www.neuro.uni-jena.de/cat/) for SPM12.

The VBM pipeline consists of several stages: tissue segmentation, spatial normalization to a standard Montreal Neurological

Institute template, modulation, and smoothing, which have been extensively described (Kurth et al., 2015). CAT12 has been suggested to provide more robust and accurate results compared with other VBM pipelines (Farokhian et al., 2017).

For each subject, the normalized and modulated gray matter map was used to extract the average between left and right gray matter insular volume (expressed as percentage of gray matter in that region) by applying a binary mask from the Automated Anatomical Labeling atlas. Insular volume was chosen as structural imaging biomarker because the insula has been shown to be the first region to be involved in presymptomatic mutation carriers (Rohrer et al., 2015).

FLAIR scans were processed with the lesion prediction algorithm (Schmidt, 2017) implemented in the Lesion Segmentation Toolbox (v.2.0.15) (www.statistical-modelling.de/lst.html) for SPM12. We considered the total WMH volume (expressed in milliliters, mL) as a measure of white matter burden, as it has been shown to be increased in patients bearing a *GRN* mutation (Le Ber et al., 2008; Paternicò et al., 2016; Pietroboni et al., 2011; Sudre et al., 2017).

2.4. Biochemical analyses

Progranulin levels were tested with a specific ELISA kit (AdipoGen, Korea), using polyclonal specific antibodies, in patients with *GRN* mutation and in their respective family members. According to the manufacturer's protocol, the test has a 5.1% coefficient of variation within an assay (intra-assay precision) and 6.4% coefficient of variation precision between assays (interassay precision) (Galimberti et al., 2018). The cutoff of 61.55 ng/mL has shown high specificity and sensitivity in identifying mutation carriers among unaffected subjects and patients attending a memory clinic (Ghidoni et al., 2012).

2.5. Neurophysiological measures

TMS was performed with a figure-of-8 coil (each loop diameter 70 mm) connected to a Magstim Bistim^2 system (Magstim Company, Oxford, UK), as previously reported (Benussi et al., 2017). The magnetic stimuli had a monophasic current waveform (rise time of 100 μs, decaying back to zero over 800 μs). Motor-evoked potentials (MEPs) were recorded from the right first dorsal interosseous muscle through surface Ag/AgCl electrodes placed in a belly-tendon montage and acquired using a BIOPAC MP-150 electromyograph (BIOPAC Systems Inc, Santa Barbara, CA, USA).

The TMS coil was held tangentially over the scalp region corresponding to the primary hand motor area contralateral to the target muscle, with the coil handle pointed 45° posteriorly and laterally to the sagittal plane. The motor hot spot was defined as the location where TMS consistently produced the largest MEP size at 120% of the resting motor threshold (rMT) in the target muscle. rMT was defined as the minimal stimulus intensity needed to produce MEPs with an amplitude of at least 50 μV in 5 of 10 consecutive trails during complete muscle relaxation, which was controlled by visually checking the absence of electromyography activity at high-gain amplification (Rossini et al., 2015).

Short-interval intracortical inhibition (SICI) and intracortical facilitation (ICF), which partially reflect $GABA_A$ergic and glutamatergic neurotransmissions, respectively, were studied at rest via a paired-pulse paradigm, delivered in a conditioning-test design with the conditioning stimulus (CS) set at an intensity of 70% of the rMT, while the test stimulus (TS) was adjusted to evoke an MEP approximately 1 mV peak-to-peak in the relaxed dorsal interosseous muscle. Different interstimulus intervals (ISIs) between the CS and TS were used to investigate preferentially both SICI (1, 2, 3, 5 ms) and ICF (7, 10, 15 ms) (Kujirai et al., 1993; Ziemann et al., 1996).

Long-interval intracortical inhibition (LICI), which partially reflects $GABA_B$ergic transmission, was elicited by applying 2 suprathreshold stimuli at long ISIs (50, 100, 150 ms), with the CS set at 130% of the rMT preceding the TS, adjusted to evoke an MEP of approximately 1 mV peak-to-peak (Valls-Solé et al., 1992).

Ten stimuli were delivered for each ISI for all stimulation paradigms and 14 control MEPs in response to the TS alone were recorded, for each paradigm, in all participants in a pseudo-randomized sequence. The amplitude of the conditioning MEPs was expressed as a ratio of the mean unconditioned response. The intertrial interval was set at 5 seconds (±10%). SICI, ICF, and LICI protocols were performed in a randomized order. Throughout the experiment, complete muscle relaxation was monitored by audio-visual feedback where appropriate. If quality of study data was degraded by patient movement, the protocol was recommenced, and the initial data discarded. Trials were discarded if electromyographic activity exceeded 100 μV in the 250 ms before TMS delivery. All patients were able to understand instructions and obtain full muscle relaxation.

2.6. Statistical analysis

Neuropsychological, biochemical, neuroimaging, and neurophysiological biomarkers were compared as a function of estimated years from expected symptom onset between mutation carriers and noncarriers. Linear mixed models were used to model each marker as a function of estimated years at symptom onset and mutation status (mutation carrier vs. noncarrier). As previously reported, nonlinear changes, as quadratic and cubic relations, for each measure, were expected over time (Rohrer et al., 2015). Accordingly, possible 2-factor, 3-factor interaction terms along with 2nd and 3rd order estimated years at symptom onset terms were examined to reach a final model that fitted the data well. A penalized likelihood method (Bayesian Information Criterion) was also considered to evaluate the model fit. Considering that some participants were recruited from the same family, a random effect was included in the mixed model to account for the family affiliation.

Average values were predicted from the mixed-effects models for each group (mutation carriers and noncarriers), and approximate Student's t-test were used to determine whether marker values differed at certain age points (every 5 years). Individual values of participants were not displayed in figures to prevent disclosure of genetic status. Statistical significance was assumed at $p < 0.05$. Data analyses were carried out using SPSS 21.0 software.

3. Results

3.1. Participants

We analyzed 186 participants, consisting of 113 mutation carriers and 73 noncarriers. Demographic characteristics of included

Table 1
Demographic characteristics of included participants

Characteristic	Carriers (n = 113)	Noncarriers (n = 73)
Age (y)	54.8 ± 13.2	43.6 ± 13.7
Sex (% female)	66 (58.4%)	47 (64.4%)
Education (y)	10.5 ± 4.2	11.8 ± 3.9
Cognitive status (%)		
Asymptomatic	52 (46.0%)	73 (100%)
Symptomatic	61 (54.0%)	0 (0%)

participants are reported in Table 1. Of the 113 mutation carriers (14 *C9orf72* and 99 *GRN*), 42 were asymptomatic (4 *C9orf72* and 48 *GRN*) and 61 were symptomatic (10 *C9orf72* and 51 *GRN*). The mean age of expected symptom onset was 60.7 ± 8.8.

3.2. Neuropsychological assessment

Behavioral symptoms were assessed with the Cambridge Behavioural Inventory-Revised version, with scores ranging from 0 (no behavioral symptoms) to 180 (maximal behavioral symptoms). Significant differences were observed between mutation carriers and noncarriers 5 years before expected symptom onset (see Table 2, Fig. 1A). General cognitive functions were evaluated with the Mini-Mental State Examination, with scores ranging from 30 (no impairment) to 0 (severe impairment). Significant differences were observed at 5 years before expected symptom onset (see Table 2, Fig. 1B). Cognitive processing speed was evaluated with the Trial Making Test part A, with a maximum score of 150 seconds (severe impairment). Significant differences were detected at 5 years before expected symptom onset between mutation carriers and noncarriers

Table 2
Cognitive, biochemical, imaging, and neurophysiological estimates in mutation carriers and noncarriers

Variable	Estimated years from expected symptom onset								
	−30	−25	−20	−15	−10	−5	0	5	10
Cambridge behavioural inventory-revised (score)									
Noncarriers	1.2	1.7	4.4	7.4	8.2	10.4	12.6	9.2	11.3
Carriers	0.8	1.2	5.5	6.9	10.7	27.8	49.8	50.3	46.7
Difference	−0.38 ± 0.6	−0.5 ± 0.9	1.1 ± 1.2	0.7 ± 1.2	2.5 ± 3.4	17.4 ± 4.3[c]	37.1 ± 4.5[c]	41.1 ± 3.2[c]	35.4 ± 4.7[c]
Mini-Mental State Examination (score)									
Noncarriers	29.6	29.6	29.6	29.4	29.3	28.4	27.7	28.6	28.8
Carriers	30.2	30.0	29.5	29.1	28.4	25.8	19.7	19.1	17.3
Difference	0.52 ± 0.2[a]	0.39 ± 0.2[a]	−0.1 ± 0.2	−0.3 ± 0.2	−0.9 ± 0.8	2.5 ± 0.9[c]	7.9 ± 1.1[c]	9.6 ± 1.0[c]	11.5 ± 2.2[c]
Trial making test part A (s)									
Noncarriers	23.2	20.9	24.1	30.8	35.6	43.2	49.5	41.1	44.5
Carriers	23.4	23.0	26.1	31.5	40.9	59.8	86.3	91.6	118.6
Difference	0.2 ± 2.2	2.1 ± 1.7	2.0 ± 1.7	0.7 ± 3.4	5.3 ± 8.4	16.6 ± 5.2[c]	36.8 ± 9.1[c]	50.4 ± 8.3[c]	80.4 ± 17.6[c]
Insular gray matter (%)									
Noncarriers	0.57	0.56	0.55	0.52	0.51	0.53	0.47	0.47	0.45
Carriers	0.56	0.56	0.54	0.53	0.47	0.45	0.37	0.36	0.32
Difference	−0.01 ± 0.02	0.00 ± 0.01	−0.00 ± 0.01	0.02 ± 0.02	−0.04 ± 0.02	−0.07 ± 0.03[c]	−0.10 ± 0.01[c]	−0.11 ± 0.01[c]	−0.13 ± 0.01[c]
White matter hyperintensities (volume, mL)									
Noncarriers	0.03	0.11	0.19	0.30	0.49	0.47	0.31	0.33	1.23
Carriers	0.07	0.25	0.79	1.41	3.14	4.75	14.81	15.10	12.34
Difference	0.04 ± 0.08	0.13 ± 0.10	0.61 ± 0.13[a]	1.10 ± 0.17[c]	2.65 ± 0.35[c]	4.28 ± 0.93[c]	14.50 ± 1.55[c]	14.77 ± 1.48[c]	11.11 ± 2.75[b]
Plasma progranulin (ng/mL)									
Noncarriers	142.7	148.8	157.4	151.0	185.9	184.7	135.0	166.3	160.0
Carriers	30.5	35.6	40.3	41.1	45.4	36.5	41.5	49.3	66.5
Difference	−112.3 ± 11.0[c]	−113.1 ± 13.7[c]	−117.1 ± 11.6[c]	−110.0 ± 13.5[c]	−140.4 ± 21.1[c]	−148.2 ± 27.6[b]	−93.5 ± 9.5[c]	−1117.6 ± 17.7[c]	−93.5 ± 28.0[b]
Average short-interval intracortical inhibition (SICI)									
Noncarriers	20.7	17.6	16.4	15.6	13.9	19.4	23.9	21.3	20.7
Carriers	26.8	29.1	35.4	36.8	37.4	49.4	75.4	75.1	64.6
Difference	6.0 ± 2.3	12.2 ± 2.0[c]	19.0 ± 2.3[c]	21.2 ± 2.3[c]	23.6 ± 3.0[c]	30.0 ± 7.0[a]	51.5 ± 1.6[c]	53.8 ± 1.8[c]	43.9 ± 4.0[c]
Average intracortical facilitation (ICF)									
Noncarriers	148.4	152.2	150.9	148.9	150.0	145.4	137.5	140.8	142.1
Carriers	117.7	118.3	108.7	102.9	99.6	96.3	88.1	87.4	87.6
Difference	−30.6 ± 3.5[c]	−33.9 ± 2.8[c]	−42.3 ± 3.2[c]	−46.0 ± 2.1[c]	−50.4 ± 0.8[c]	−49.1 ± 4.3[c]	−49.3 ± 1.9[c]	−53.3 ± 1.4[c]	−54.5 ± 1.1[c]
Average long-interval intracortical inhibition (LICI)									
Noncarriers	28.7	28.5	21.0	14.5	17.3	29.0	26.4	20.7	19.0
Carriers	34.6	37.2	53.4	63.6	69.7	95.7	109.7	106.1	87.9
Difference	5.9 ± 6.1	8.7 ± 6.1	32.3 ± 7.2[c]	49.1 ± 4.3[c]	52.4 ± 4.9[c]	66.8 ± 19.7[a]	83.3 ± 9.2[c]	85.5 ± 6.9[c]	68.9 ± 14.3[c]

Estimates are reported as average ± standard error for the predicted difference between mutation carriers and noncarriers, which were obtained with the use of mixed-effects models.

[a] $p < 0.05$.
[b] $p < 0.01$.
[c] $p < 0.001$.

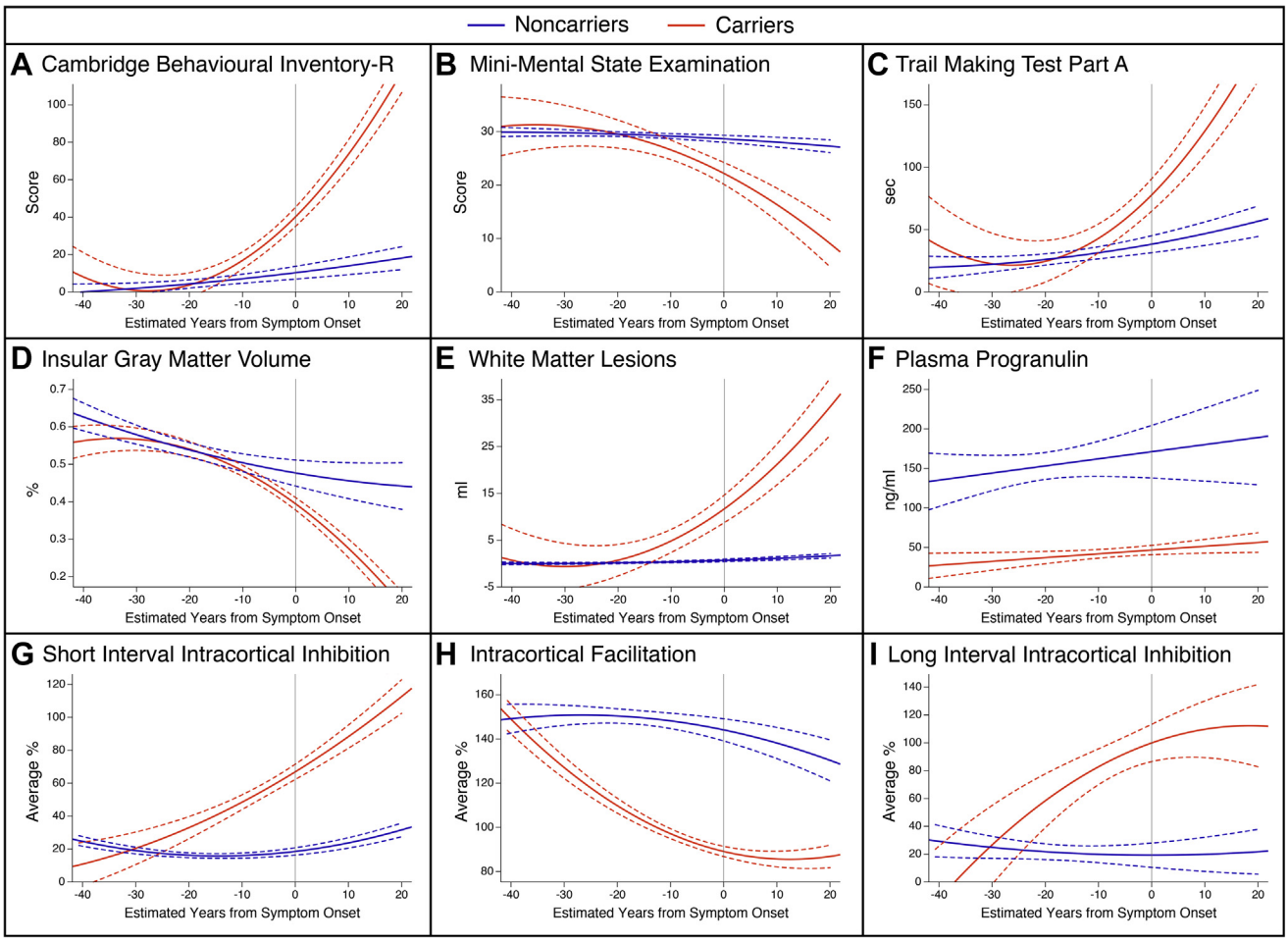

Fig. 1. Cognitive, biochemical, imaging, and neurophysiological estimates in mutation carriers versus noncarriers, according to estimated years from expected symptom onset. (A) Cambridge behavioural inventory-revised; (B) Mini-mental state examination; (C) Trail making test part A; (D) insular gray matter volume (%); (E) white matter lesions (mL); (F) plasma progranulin (ng/mL); (G) average short-interval intracortical inhibition (interstimulus interval [ISI] 1, 2, 3 ms); (H) average intracortical facilitation (ISI 7, 10, 15 ms); (I) average long-interval intracortical inhibition (ISI 50, 100, 150 ms). Dashed lines represent 99.9% confidence intervals of the fitted curves.

(see Table 2, Fig. 1C). As reported, we observed a modest age-related increase in execution times also in noncarriers.

3.3. Brain imaging

A significant decrease was observed in average insular gray matter volume in mutation carriers compared with noncarriers at 5 years before expected symptom onset (see Table 2, Fig. 1D). In patients bearing a *GRN* mutation, a significant increase in WMH was observed at 20 years before expected symptom onset compared with their respective noncarrier family members (see Table 2, Fig. 1E).

3.4. Biochemical analyses

Plasma progranulin levels were tested only in patients bearing a *GRN* null mutation and their respective family members (79 carriers and 50 noncarriers). In mutation carriers, progranulin levels were already reduced at more than 30 years before expected symptom onset compared with noncarriers (see Table 2, Fig. 1F).

3.5. Neurophysiological measures

SICI, which indirectly and partially depends on $GABA_A$ergic transmission, was significantly reduced in mutation carriers at 25 years before expected symptom onset as compared with noncarriers (see Table 2, Fig. 1G).

ICF, which partially reflects glutamatergic transmission, was significantly reduced at 30 years before expected symptom onset in mutation carriers, as compared with noncarriers (see Table 2, Fig. 1H). LICI, which partially depends on $GABA_B$ergic transmission, was significantly reduced at 20 years before expected symptom onset in carriers as compared with noncarriers (see Table 2, Fig. 1I).

All intracortical connectivity measured showed a progressive decrease as a function of estimated years from expected symptom onset, at least until clinical symptom onset.

3.6. Combined model

A combined model was constructed with normalized differences between mutation carriers and noncarriers to evaluate the different order, rate, and relationship between clinical, cognitive, imaging, biochemical, and neurophysiological changes in genetic FTD (see Fig. 2). Already at more than 30 years before expected symptom onset, a significant decrease in plasma progranulin levels was observed in *GRN* mutation carriers, whereas at more than 30 years, initial changes in ICF were detected. Nearly 10 years later, 25 years before expected symptom onset, a decrease in SICI and subsequently LICI becomes manifest. An increase in white matter lesions was detected approximately 15 years before expected symptom

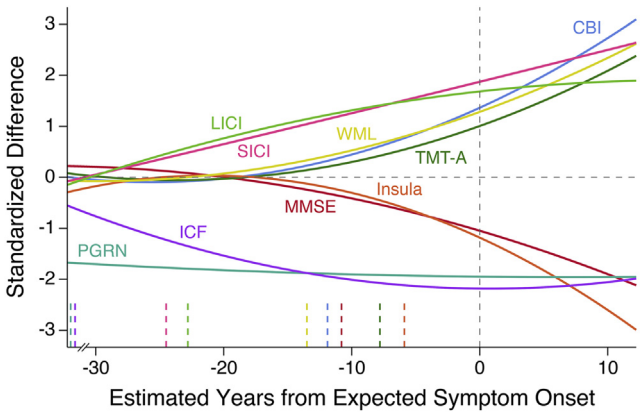

Fig. 2. Comparison of standardized cognitive, biochemical, imaging, and neurophysiological changes as a function of estimated years from expected symptom onset. Standardized differences between mutation carriers and noncarriers are shown versus estimated years from expected symptom onset and plotted with a fitted curve. The time at which the upper 99.9% confidence intervals for each curve crosses zero on the y-axis (i.e., the point at which a significant ($p < 0.001$) difference exists between mutation carriers and noncarriers) is shown on the x-axis. Abbreviations: CBI, Cambridge behavioural inventory-revised; ICF, average intracortical facilitation (ISI 7, 10, 15 ms); Insula, Insular gray matter volume; LICI, average long-interval intracortical inhibition (ISI 50, 100, 150 ms); MMSE, Mini-Mental State Examination; PGRN, plasma progranulin; SICI, average short-interval intracortical inhibition (ISI 1, 2, 3 ms); TMT-A, Trail making test part A; WML, white matter lesions.

onset, followed by a global cognitive impairment starting 10 to 5 years before expected symptom onset. A significant decrease in insular gray matter density in mutation carriers was observed approximately 5 years before expected symptom onset.

4. Discussion

In the present study, we have estimated the timing and relationship of different biomarkers in genetic FTD, describing the natural disease course from the earliest abnormalities to symptom onset. We have reported that biological changes and ICF transmission abnormalities, which partially reflect glutamatergic transmission, significantly antecede the emergence of clinical symptoms of at least 3 decades. These are followed by intracortical inhibition transmission deficits, which primarily depend on $GABA_A$ergic transmission, detected approximately 2 decades before expected symptom onset, then followed by an increase of white matter lesions, structural brain atrophy, and cognitive impairment.

These conclusions reflect and corroborate previous findings in genetic FTD, including results from the Genetic Frontotemporal dementia Initiative study, which identified significant differences of brain structural changes between mutation carriers and noncarriers at the earliest time point 10 years before expected symptom onset and cognitive decline and behavioral disturbances up to 5 years before expected symptom onset (Rohrer et al., 2015). Nevertheless, what has emerged from this study is that the onset of structural and cognitive changes may be preceded by alterations of intracortical connectivity measures, which have been shown to indirectly and partially reflect specific neurotransmitter deficits. In this view, a recent reappraisal of the neurotransmitter literature has shed important implications on the pharmacological abnormalities associated with FTD in terms of regional changes in neurotransmitter synthesis, release, reuptake, catabolism, and synaptic binding (Murley and Rowe, 2018).

Regarding glutamatergic transmission, several studies have shown a decrease in glutamatergic neurons in the frontal and temporal cortices and in the thalamus (Ferrer, 1999; Procter et al., 1999), with magnetic resonance spectroscopy studies finding a decrease in glutamate/glutamine levels in the frontal and temporal lobes in FTD (Ernst et al., 1997). In the same view, a reduced ICF, which is thought to represent a net facilitation most likely mediated by glutamatergic NMDA receptors (Kujirai et al., 1993; Ziemann et al., 1996), has been observed both in patients with sporadic (Benussi et al., 2017) and genetic FTD (Benussi et al., 2016; Gazzina et al., 2018) in progressive supranuclear palsy and corticobasal syndrome (Benussi et al., 2018).

Regarding GABAergic transmission, initial studies have shown that a subgroup of GABAergic neurons that bind calbinidin-D28k are reduced in the upper neocortical layers of the frontal and temporal cortices in FTD (Ferrer, 1999), while gamma oscillations and coherence, which reflect GABA inhibition, are reduced between the frontal lobes of patients with behavioral variant FTD (Hughes et al., 2013). These findings are corroborated by reports of the toxic effects mediated by tau and trans-activation response element DNA-binding protein 43 on GABAergic interneurons, leading to a loss of GABAergic function in animal models (Levenga et al., 2013; Yamashita and Kwak, 2014).

Concerning TMS studies, the evaluation of SICI and LICI has shown to reflect short-lasting postsynaptic inhibition mediated through the $GABA_A$ and $GABA_B$ receptors, respectively, at the level of local interneurons (Kujirai et al., 1993; Valls-Solé et al., 1992; Ziemann et al., 2015). Indeed, a few studies have shown a significant decrease of SICI in patients with sporadic FTD (Benussi et al., 2017; Burrell et al., 2011), in presymptomatic and symptomatic *GRN* carriers (Benussi et al., 2016; Gazzina et al., 2018), in symptomatic *C9orf72* carriers (Geevasinga et al., 2015), and in progressive supranuclear palsy/corticobasal syndrome (Benussi et al., 2018; Burrell et al., 2014; Frasson et al., 2003; Pal et al., 2008).

The disruption of specific neurotransmitter circuits is of particular relevance because it has been shown that the GABA-glutamate interaction supports precisely tuned oscillatory dynamics of neural circuits, which are the basis for cognition (Bastos et al., 2012). These findings, here observed more than 30 years before symptom onset in presymptomatic carriers, further support the concept of a major role of a neurodevelopmental component to a dementing condition that has been predominantly considered to be a disease of aging (Geschwind et al., 2001).

Understanding the time in which different biomarkers change is critical for constructing clinical and pharmacological studies designed to prevent or slow disease progression and for a more refined insight into the pathophysiology of the disease. In this view, we argue for the use of different and specific biomarkers that should be used to answer precise clinical issues. For example, if the main target is to identify the conversion to dementia, presumably a structural imaging or cognitive biomarker would be most suitable. On the other hand, if we believe that targeting the disease in the very initial phases, when the burden of pathological accumulations is still negligible and possibly reversible, other biomarkers as intracortical connectivity measures or plasma progranulin levels might be more supportive. Furthermore, these results highlight how plasma progranulin levels are more useful as a "status" biomarker, predicting the presence or absence of *GRN* mutations in asymptomatic subjects and not as a "progression" biomarker, with levels not changing significantly during disease progression. This finding is supported by previous studies in which plasma progranulin levels have shown not to correlate with brain atrophy (Galimberti et al., 2018). On the other hand, neurophysiological biomarkers are to be considered as "progression" biomarkers, particularly in the early disease stages, followed by clinical and neuroimaging changes.

A crucial strength of this study, compared with previous studies on genetic FTD, is that it includes both cross-sectional and longitudinal data of single patients, comparing different types of

biological markers into a single model, improving previous models in which the progression of biomarkers changes could not be assessed within individuals. We acknowledge that our study entails some limitations. The lack of patients with *MAPT* and other causative mutations could hinder generalizations to all forms of inherited FTD, which should be made with caution. Nevertheless, including only patients with an underlying trans-activation response element DNA-binding protein 43 pathology, as in *GRN* and *C9orf72* mutations, could reduce variability and increase consistency in these findings. Another limitation, as suggested for similar studies on the genetic forms of dementia (Bateman et al., 2012; Rohrer et al., 2015), is the method implemented for estimation of age at disease onset for presymptomatic carriers, considering the important variability in age at onset within a family in all types of FTD mutations and the possible role of anticipation in *C9orf72* expansion carriers (Van Mossevelde et al., 2017). Moreover, although the clinical and pathological phenotypes of genetic FTD are similar to those of sporadic FTD, the generalizability of the nature and sequence of brain changes in genetic FTD remains to be determined for sporadic FTD.

In conclusion, our findings suggest that several available biomarkers can show different aspects and rates of decline, possibly correlated with the underlying physiopathological process, that arise decades before the onset of clinical symptoms. The use of different biomarkers must be thus tailored to the specific clinical question awaiting to be answered.

Disclosure

The authors have no actual or potential conflicts of interest.

Acknowledgements

This study was supported by grants from "AIRAlzh Onlus" and "ANCC-COOP" issued to VC; Italian Ministry of Health (Ricerca Corrente) issued to LB and RG; and partially supported by a grant from the Italian Ministry of Health (GR-2013-02357415) issued to MC.

Authors' contribution: AB and BB designed the study. AB, SG, EP, MC, SA, VD, VC, MSC, AA, AM, LB, RG, AP, and BB recruited patients. AB, SG, EP, MC, and BB performed experiments and analyzed the data. AB, SG, EP, and BB evaluated the data and cowrote the article. AB, SG, EP, MC, SA, VD, VC, MSC, AA, AM, LB, RG, AP, and BB contributed to revising the article for intellectual content.

References

Bastos, A.M., Usrey, W.M., Adams, R.A., Mangun, G.R., Fries, P., Friston, K.J., 2012. Canonical microcircuits for predictive coding. Neuron 76, 695–711.

Bateman, R.J., Xiong, C., Benzinger, T.L.S., Fagan, A.M., Goate, A., Fox, N.C., Marcus, D.S., Cairns, N.J., Xie, X., Blazey, T.M., Holtzman, D.M., Santacruz, A., Buckles, V., Oliver, A., Moulder, K., Aisen, P.S., Ghetti, B., Klunk, W.E., McDade, E., Martins, R.N., Masters, C.L., Mayeux, R., Ringman, J.M., Rossor, M.N., Schofield, P.R., Sperling, R.A., Salloway, S., Morris, J.C., Dominantly Inherited Alzheimer Network, 2012. Clinical and biomarker changes in dominantly inherited Alzheimer's disease. N. Engl. J. Med. 367, 795–804.

Benussi, A., Cosseddu, M., Filareto, I., Dell'Era, V., Archetti, S., Sofia Cotelli, M., Micheli, A., Padovani, A., Borroni, B., 2016. Impaired long-term potentiation-like cortical plasticity in presymptomatic genetic frontotemporal dementia. Ann. Neurol. 80, 472–476.

Benussi, A., Dell'Era, V., Cantoni, V., Ferrari, C., Caratozzolo, S., Rozzini, L., Alberici, A., Padovani, A., Borroni, B., 2018. Discrimination of atypical parkinsonisms with transcranial magnetic stimulation. Brain Stimul. 11, 366–373.

Benussi, A., Di Lorenzo, F., Dell'Era, V., Cosseddu, M., Alberici, A., Caratozzolo, S., Cotelli, M.S., Micheli, A., Rozzini, L., Depari, A., Flammini, A., Ponzo, V., Martorana, A., Caltagirone, C., Padovani, A., Koch, G., Borroni, B., 2017. Transcranial magnetic stimulation distinguishes Alzheimer disease from frontotemporal dementia. Neurology 89, 665–672.

Benussi, A., Padovani, A., Borroni, B., 2015. Phenotypic heterogeneity of monogenic frontotemporal dementia. Front. Aging Neurosci. 7, 171.

Burrell, J.R., Hornberger, M., Vucic, S., Kiernan, M.C., Hodges, J.R., 2014. Apraxia and motor dysfunction in corticobasal syndrome. PLoS One 9, e92944.

Burrell, J.R., Kiernan, M.C., Vucic, S., Hodges, J.R., 2011. Motor Neuron dysfunction in frontotemporal dementia. Brain 134, 2582–2594.

Ernst, T., Chang, L., Melchor, R., Mehringer, C.M., 1997. Frontotemporal dementia and early Alzheimer disease: differentiation with frontal lobe H-1 MR spectroscopy. Radiology 203, 829–836.

Farokhian, F., Beheshti, I., Sone, D., Matsuda, H., 2017. Comparing CAT12 and VBM8 for detecting brain morphological abnormalities in temporal lobe epilepsy. Front. Neurol. 8, 428.

Ferrer, I., 1999. Neurons and their dendrites in frontotemporal dementia. Dement Geriatr. Cogn. Disord. 10, 55–60.

Frasson, E., Bertolasi, L., Bertasi, V., Fusina, S., Bartolomei, L., Vicentini, S., Rizzuto, N., Priori, A., 2003. Paired transcranial magnetic stimulation for the early diagnosis of corticobasal degeneration. Clin. Neurophysiol. 114, 272–278.

Galimberti, D., Fumagalli, G.G., Fenoglio, C., Cioffi, S.M.G., Arighi, A., Serpente, M., Borroni, B., Padovani, A., Tagliavini, F., Masellis, M., Tartaglia, M.C., Van Swieten, J., Meeter, L., Graff, C., de Mendonça, A., Bocchetta, M., Rohrer, J.D., Scarpini, E., 2018. Progranulin plasma levels predict the presence of GRN mutations in asymptomatic subjects and do not correlate with brain atrophy: results from the GENFI study. Neurobiol. Aging 62, 245.e9–245.e12.

Gazzina, S., Benussi, A., Premi, E., Paternicò, D., Cristillo, V., Dell'Era, V., Cosseddu, M., Archetti, S., Alberici, A., Gasparotti, R., Padovani, A., Borroni, B., 2018. Neuroanatomical correlates of transcranial magnetic stimulation in presymptomatic granulin mutation carriers. Brain Topogr. 31, 488–497.

Geevasinga, N., Menon, P., Nicholson, G.A., Ng, K., Howells, J., Kril, J.J., Yiannikas, C., Kiernan, M.C., Vucic, S., 2015. Cortical function in asymptomatic carriers and patients with C9orf72Amyotrophic lateral sclerosis. JAMA Neurol. 72, 1268.

Geschwind, D.H., Robidoux, J., Alarcón, M., Miller, B.L., Wilhelmsen, K.C., Cummings, J.L., Nasreddine, Z.S., 2001. Dementia and neurodevelopmental predisposition: cognitive dysfunction in presymptomatic subjects precedes dementia by decades in frontotemporal dementia. Ann. Neurol. 50, 741–746.

Ghidoni, R., Benussi, L., Glionna, M., Franzoni, M., Binetti, G., 2008. Low plasma progranulin levels predict progranulin mutations in frontotemporal lobar degeneration. Neurology 71, 1235–1239.

Ghidoni, R., Stoppani, E., Rossi, G., Piccoli, E., Albertini, V., Paterlini, A., Glionna, M., Pegoiani, E., Agnati, L.F., Fenoglio, C., Scarpini, E., Galimberti, D., Morbin, M., Tagliavini, F., Binetti, G., Benussi, L., 2012. Optimal plasma progranulin cutoff value for predicting null progranulin mutations in neurodegenerative diseases: a multicenter Italian study. Neurodegener. Dis. 9, 121–127.

Gorno-Tempini, M.L., Hillis, A.E., Weintraub, S., Kertesz, A., Mendez, M., Cappa, S.F., Ogar, J.M., Rohrer, J.D., Black, S., Boeve, B.F., Manes, F., Dronkers, N.F., Vandenberghe, R., Rascovsky, K., Patterson, K., Miller, B.L., Knopman, D.S., Hodges, J.R., Mesulam, M.-M., Grossman, M., 2011. Classification of primary progressive aphasia and its variants. Neurology 76, 1006–1014.

Hughes, L.E., Ghosh, B.C.P., Rowe, J.B., 2013. Reorganisation of brain networks in frontotemporal dementia and progressive supranuclear palsy. Neuroimage Clin. 2, 459–468.

Kujirai, T., Caramia, M.D., Rothwell, J.C., Day, B.L., Thompson, P.D., Ferbert, A., Wroe, S., Asselman, P., Marsden, C.D., 1993. Corticocortical inhibition in human motor cortex. J. Physiol. 471, 501–519.

Kurth, F., Gaser, C., Luders, E., 2015. A 12-step user guide for analyzing voxel-wise gray matter asymmetries in statistical parametric mapping (SPM). Nat. Protoc. 10, 293–304.

Le Ber, I., Camuzat, A., Hannequin, D., Pasquier, F., Guedj, E., Rovelet-Lecrux, A., Hahn-Barma, V., van der Zee, J., Clot, F., Bakchine, S., Puel, M., Ghanim, M., Lacomblez, L., Mikol, J., Deramecourt, V., Lejeune, P., la Sayette de, V., Belliard, S., Vercelletto, M., Meyrignac, C., Van Broeckhoven, C., Lambert, J.-C., Verpillat, P., Campion, D., Habert, M.O., Dubois, B., Brice, A., the French research network on FTD/FTD-MND, 2008. Phenotype variability in progranulin mutation carriers: a clinical, neuropsychological, imaging and genetic study. Brain 131, 732–746.

Levenga, J., Krishnamurthy, P., Rajamohamedsait, H., Wong, H., Franke, T.F., Cain, P., Sigurdsson, E.M., Hoeffer, C.A., 2013. Tau pathology induces loss of GABAergic interneurons leading to altered synaptic plasticity and behavioral impairments. Acta Neuropathol. Commun. 1, 34.

Meeter, L.H.H., Patzke, H., Loewen, G., Dopper, E.G.P., Pijnenburg, Y.A.L., van Minkelen, R., van Swieten, J.C., 2016. Progranulin levels in plasma and cerebrospinal fluid in granulin mutation carriers. Dement Geriatr. Cogn. Disord. Extra 6, 330–340.

Murley, A.G., Rowe, J.B., 2018. Neurotransmitter deficits from frontotemporal lobar degeneration. Brain 141, 1263–1285.

Pal, P.K., Gunraj, C.A., Li, J.Y., Lang, A.E., Chen, R., 2008. Reduced intracortical and interhemispheric inhibitions in corticobasal syndrome. J. Clin. Neurophysiol. 25, 304–312.

Paternicò, D., Premi, E., Gazzina, S., Cosseddu, M., Alberici, A., Archetti, S., Cotelli, M.S., Micheli, A., Turla, M., Gasparotti, R., Padovani, A., Borroni, B., 2016. White matter hyperintensities characterize monogenic frontotemporal dementia with granulin mutations. Neurobiol. Aging 38, 176–180.

Pietroboni, A.M., Fumagalli, G.G., Ghezzi, L., Fenoglio, C., Cortini, F., Serpente, M., Cantoni, C., Rotondo, E., Corti, P., Carecchio, M., Bassi, M., Bresolin, N., Galbiati, D., Galimberti, D., Scarpini, E., 2011. Phenotypic heterogeneity of the GRN Asp22fs mutation in a large Italian kindred. J. Alzheimers Dis. 24, 253–259.

Procter, A.W., Qurne, M., Francis, P.T., 1999. Neurochemical features of frontotemporal dementia. Dement. Geriatr. Cogn. Disord. 10, 80–84.

Rascovsky, K., Hodges, J.R., Knopman, D., Mendez, M.F., Kramer, J.H., Neuhaus, J., van Swieten, J.C., Seelaar, H., Dopper, E.G.P., Onyike, C.U., Hillis, A.E., Josephs, K.A., Boeve, B.F., Kertesz, A., Seeley, W.W., Rankin, K.P., Johnson, J.K., Gorno-Tempini, M.L.,

Rosen, H., Prioleau-Latham, C.E., Lee, A., Kipps, C.M., Lillo, P., Piguet, O., Rohrer, J.D., Rossor, M.N., Warren, J.D., Fox, N.C., Galasko, D., Salmon, D.P., Black, S.E., Mesulam, M.-M., Weintraub, S., Dickerson, B.C., Diehl-Schmid, J., Pasquier, F., Deramecourt, V., Lebert, F., Pijnenburg, Y., Chow, T.W., Manes, F., Grafman, J., Cappa, S.F., Freedman, M., Grossman, M., Miller, B.L., 2011. Sensitivity of revised diagnostic criteria for the behavioural variant of frontotemporal dementia. Brain 134, 2456–2477.

Rohrer, J.D., Guerreiro, R., Vandrovcova, J., Uphill, J., Reiman, D., Beck, J., Authier, A., Ferrari, R., Fox, N.C., Mackenzie, I.R.A., Warren, J.D., de Silva, R., Holton, J., Revesz, T., Hardy, J., Mead, S., Rossor, M.N., 2009. The heritability and genetics of frontotemporal lobar degeneration. Neurology 73, 1451–1456.

Rohrer, J.D., Nicholas, J.M., Cash, D.M., Van Swieten, J., Dopper, E., Jiskoot, L., van Minkelen, R., Rombouts, S.A., Cardoso, M.J., Clegg, S., Espak, M., Mead, S., Thomas, D.L., De Vita, E., Masellis, M., Black, S.E., Freedman, M., Keren, R., MacIntosh, B.J., Rogaeva, E., Tang-Wai, D., Tartaglia, M.C., Laforce, R., Tagliavini, F., Tiraboschi, P., Redaelli, V., Prioni, S., Grisoli, M., Borroni, B., Padovani, A., Galimberti, D., Scarpini, E., Arighi, A., Fumagalli, G., Rowe, J.B., Coyle-Gilchrist, I., Graff, C., Fallström, M., Jelic, V., Ståhlbom, A.K., Andersson, C., Thonberg, H., Lilius, L., Frisoni, G.B., Pievani, M., Bocchetta, M., Benussi, L., Ghidoni, R., Finger, E., Sorbi, S., Nacmias, B., Lombardi, G., Polito, C., Warren, J.D., Ourselin, S., Fox, N.C., Rossor, M.N., Binetti, G., 2015. Presymptomatic cognitive and neuroanatomical changes in genetic frontotemporal dementia in the Genetic Frontotemporal dementia Initiative (GENFI) study: a cross-sectional analysis. Lancet Neurol. 14, 253–262.

Rossini, P.M., Burke, D., Chen, R., Cohen, L.G., Daskalakis, Z., Di Iorio, R., Di Lazzaro, V., Ferreri, F., Fitzgerald, P.B., George, M.S., Hallett, M., Lefaucheur, J.P., Langguth, B., Matsumoto, H., Miniussi, C., Nitsche, M.A., Pascual-Leone, A., Paulus, W., Rossi, S., Rothwell, J.C., Siebner, H.R., Ugawa, Y., Walsh, V., Ziemann, U., 2015. Non-invasive electrical and magnetic stimulation of the brain, spinal cord, roots and peripheral nerves: basic principles and procedures for routine clinical and research application. An updated report from an I.F.C.N. Committee. Clin. Neurophysiol. 126, 1071–1107.

Schmidt, P., 2017. Bayesian inference for structured additive regression models for large-scale problems with applications to medical imaging. Dissertation, LMU München: Faculty of Mathematics, Computer Science and Statistics.

Sudre, C.H., Bocchetta, M., Cash, D., Thomas, D.L., Woollacott, I., Dick, K.M., Van Swieten, J., Borroni, B., Galimberti, D., Masellis, M., Tartaglia, M.C., Rowe, J.B., Graff, C., Tagliavini, F., Frisoni, G., Laforce Jr., R., Finger, E., de Mendonça, A., Sorbi, S., Ourselin, S., Cardoso, M.J., Rohrer, J.D., 2017. White matter hyperintensities are seen only in GRN mutation carriers in the GENFI cohort. Neuroimage Clin. 15, 171–180.

The Lund and Manchester Groups, 1994. Clinical and neuropathological criteria for frontotemporal dementia. The lund and manchester groups. J. Neurol. Neurosurg. Psychiatry 57, 416–418.

Valls-Solé, J., Pascual-Leone, A., Wassermann, E.M., Hallett, M., 1992. Human motor evoked responses to paired transcranial magnetic stimuli. Electroencephalogr. Clin. Neurophysiol. 85, 355–364.

Van Mossevelde, S., van der Zee, J., Gijselinck, I., Sleegers, K., De Bleecker, J., Sieben, A., Vandenberghe, R., Van Langenhove, T., Baets, J., Deryck, O., Santens, P., Ivanoiu, A., Willems, C., Bäumer, V., Van den Broeck, M., Peeters, K., Mattheijssens, M., De Jonghe, P., Cras, P., Martin, J.-J., Cruts, M., De Deyn, P.P., Engelborghs, S., Van Broeckhoven, C., for the Belgian Neurology (BELNEU) Consortium, 2017. Clinical evidence of disease anticipation in families segregating a C9orf72Repeat expansion. JAMA Neurol. 74, 445–452.

Yamashita, T., Kwak, S., 2014. The molecular link between inefficient GluA2 Q/R site-RNA editing and TDP-43 pathology in motor neurons of sporadic amyotrophic lateral sclerosis patients. Brain Res. 1584, 28–38.

Ziemann, U., Rothwell, J.C., Ridding, M.C., 1996. Interaction between intracortical inhibition and facilitation in human motor cortex. J. Physiol. 496, 873–881.

Ziemann, U., Reis, J., Schwenkreis, P., Rosanova, M., Strafella, A., Badawy, R., Müller-Dahlhaus, F., 2015. TMS and drugs revisited 2014. Clin. Neurophysiol. 126, 1847–1868.